Published in final edited form as:

Nature. 2020 April ; 580(7801): 76–80. doi:10.1038/s41586-020-2131-1.

Discovery and Characterization of Acridine Radical Photoreductants

Ian A. MacKenzie[1,‡], **Leifeng Wang**[1,‡], **Nicholas P. R. Onuska**[1,‡], **Olivia F. Williams**[1], **Khadiza Begam**[2], **Andrew M. Moran**[1], **Barry D. Dunietz**[3], **David A. Nicewicz**[1]

[1]Department of Chemistry, University of North Carolina at Chapel Hill, Venable Laboratories, Chapel Hill, NC 27599-3290, USA

[2]Department of Physics, Kent State University, Kent, OH 44243, USA

[3]Department of Chemistry and Biochemistry, Kent State University, Kent, OH 44243, USA

Summary:

Photoinduced electron transfer (PET) is a phenomenon wherein the absorption of light by a chemical species provides an energetic driving force for an electron transfer reaction.[1–4] This mechanism is relevant in many areas of chemistry, including the study of natural and artificial photosynthesis, photovoltaics, and photosensitive materials. In recent years, research in the area of photoredox catalysis has leveraged PET for the catalytic generation of both neutral and charged organic free radical species. These technologies have enabled a wide range of previously inaccessible chemical transformations and have seen widespread utilization in both academic and industrial settings. These reactions are often catalyzed by visible-light absorbing organic molecules or transition-metal complexes of ruthenium, iridium, chromium, or copper.[5,6] While a wide variety of closed shell organic molecules have been shown to behave as competent electron transfer catalysts in photoredox reactions, there are only limited reports of PET reactions involving *neutral organic radicals* as an excited state donor or acceptor. This is perhaps somewhat unsurprising in light of previously reported doublet excited state lifetimes for neutral organic radicals, which are typically several orders of magnitude shorter than singlet lifetimes for known transition metal photoredox catalysts.[7–11] Herein we document the discovery, characterization, and reactivity of a neutral acridine radical with a maximum excited state oxidation potential of −3.36 V vs. SCE: significantly more reducing than elemental lithium and marking it as one of the most

Author Information Reprints and permissions information is available at www.nature.com/reprints. The authors declare no competing financial interests. Correspondence and requests for materials should be addressed to D.A.N. (nicewicz@unc.edu).

Author contributions: I.A.M. and D.A.N. were responsible for the initial conception of the project. I.A.M, L.F.W., and N.P.R.O. devised and executed all experimental work. N.P.R.O., D.A.N., K.B., B.D., O.F.W. and I.A.M. assisted in the preparation and editing of the final manuscript. O.F.W. assisted in the collection and analysis of transient absorption data. K.B., B.D., N.P.R.O. and D.A.N. were responsible for the execution and analysis of computations.

‡These authors contributed equally to this work

Data Availability

The authors declare that the data supporting the findings of this study are available within the paper and its supplementary information.

Supplementary Information is linked to the online version of the paper at www.nature.com/nature.

Competing Interests: The authors declare no competing interests.

potent chemical reductants reported.[12] Spectroscopic, computational, and chemical studies indicate that the formation of a twisted intramolecular charge transfer species enables the population of higher energy doublet excited states, leading to the observed potent photoreductant behavior. We demonstrate that this catalytically-generated PET catalyst facilitates several chemical reactions that typically require alkali metal reductants and bodes well for the adoption of this system in additional organic transformations requiring dissolving metal reductants.

Our lab, as well as others, have published numerous examples highlighting the diverse reactivity of acridinium salts, such as **Mes-Acr$^+$BF$_4^-$**, as photooxidation catalysts in the excited state (***Mes-Acr**$^+$; Figure 1A).[13] Upon absorption of visible light, the corresponding excited state of the acridinium salt is populated and may be quenched *via* electron transfer from an electrochemically-matched substrate, resulting in the formation of an acridine radical (**Mes-Acr•**; Figure 1A). In past work utilizing acridinium photoredox catalysts, this radical is typically oxidized to regenerate the parent acridinium and close a catalytic cycle. During previous mechanistic studies conducted by our laboratory, it was noted that solutions of **Mes-Acr•** generated *via* reduction of **Mes-Acr$^+$BF$_4^-$** with cobaltocene were indefinitely stable under oxygen-free conditions and possessed two major absorption features (350–400 nm and 450–550 nm; Figure 1B).[14] These observations led us to explore the photophysical behavior of this radical, with a focus on identifying potential PET behavior. Previous studies have detailed the *in situ* generation and excitation of stable cation radical and anion radical species and their use in catalytic reactions,[15–19] indicating the potential feasibility of this strategy and prompting our studies of the photophysical behavior of **Mes-Acr•**.

Upon investigation of the excited state dynamics of **Mes-Acr•**, we found that there are two main excited states, tentatively assigned as a lower energy doublet (**D$_1$**) and higher energy twisted intramolecular charge transfer state (**TICT**). The excited state energy for the doublet excited state of **Mes-Acr•** is estimated by averaging the energies of the lowest energy absorption maximum and the highest energy emission observed upon 484 nm excitation. The energy of the proposed higher order excited state is estimated by averaging the energies of the emission maximum near 490 nm and the maximum of the corresponding excitation spectrum monitored at this wavelength (see SI for full details of excited state energy calculations). Estimation of excited state energies in this fashion gives values of 2.31 eV for the energy of the proposed D_1 excited state and 2.76 eV for the corresponding higher energy excited state (Figure 1E). Using the known electrochemical potential of **Mes-Acr•**[20] the excited state oxidation potentials of these states were estimated to be −2.91 V vs. SCE and −3.36 V vs. SCE, respectively. To our knowledge, these values represent some of the most negative excited state oxidation potentials reported for an organic molecule.

Before we proceed to discuss the calculated excited state energies, we consider the key orbitals involved in the low-lying excited states. We find that the singly occupied molecular orbital (SOMO) density is localized on acridine core and the lowest unoccupied MO (LUMO+1) is localized on the *N*-phenyl ring of **Mes-Acr•** (Figure 1C). Based on this observation of small spatial overlap between these two orbitals, we expect to find a relatively low lying excitation of an intramolecular CT (charge transfer) state. To further probe the excited state behavior of **Mes-Acr•**, transient absorption experiments were performed

(Figure 1D). At early pump-probe delay times in THF, the ground state of **Mes-Acr•** is bleached (ΔA < 0) and excited state absorbance resonances (ΔA > 0) with maxima at 550 nm and ~650 nm are observed. Aromatic radical anions are known to exhibit broad absorbances in the 600–800 nm range as is aqueous solvated electron.[21–23] The observed excited state absorbance signal at ~550 nm also matches the absorbance profile expected for a general acridine exitonic structure. Simple first-order decay to the ground state occurs after ~100 ps, matching well with previously reported values for excited state lifetimes of organic radicals. TD-DFT calculations indicate that other red-shifted absorptions present are well matched with energies calculated for a general acridinium structure. These spectral features support the formation of a charge transfer state possessing both aromatic radical anion and acridinium features, as expected for the proposed TICT state.

To better understand the effect of rotation of the *N*-phenyl ring on the excited state energetics of the acridine radical, we employ the recently reported polarization consistent TD-DFT based framework for obtaining excited state energies of solvated molecular systems. The approach addresses dielectric polarization consistently by invoking the same dielectric constant in the screened range separated hybrid (SRSH) functional parameters and in the polarizable continuum mode (PCM). SRSH-PCM was benchmarked well in calculating CT state energies of solvated donor-acceptor complex and in analyzing the spectral trends of several pigments with increased accuracy where conventional TD-DFT calculations fail to reproduce the observed trends (see SI for full computational details).[24–27]

The calculated doublet excited state energies for **Mes-Acr•** agree very well (within 0.1 eV) with values estimated *via* spectroscopic measurements for both the absorption and emission spectra (Figure 1E). The lowest energy calculated D_1 state, possessing an excited state energy of 2.29 eV, agrees with the experimentally determined D_1 value of 2.31 eV. Additionally, two excited states possessing significant charge transfer character were identified and the corresponding energies were calculated to be 2.75 and 2.78 eV, matching closely with estimated spectroscopic values for the proposed TICT state energy of 2.76 eV. As such, the identified D_1 (2.29 eV) state is assigned as an untwisted exitonic state, while the calculated 2.78 eV state is assigned as a TICT state. These excited state energy values also correspond well with previously reported excited state energies for neutral radical species.[9] Additionally, visualizations of the geometries of the corresponding TICT state indicate significant rotation of the *N*-phenyl ring (36 degrees) relative to the more planarized geometry of the D_1 state, providing further evidence of the profound effects of *N*-phenyl rotation on excited state energy.

With the electronic and excited state behavior of **Mes-Acr•** elucidated, we sought to utilize this species as a catalytic reductant in a photoredox manifold. Previous work in reductive photoredox catalysis has established the reduction of aryl halides as a common benchmark reaction for these types of transformations.[15,28–30] Furthermore, the extremely potent reducing behavior of the acridine radical should enable the reduction of a wide range of electronically diverse substrates. Diisopropylamine (DIPEA) was identified as a suitable single electron reductant for the generation of **Mes-Acr•** from **Mes-Acr$^+$BF$_4^-$** *in situ*. Following excitation, **Mes-Acr$^+$BF$_4^-$** undergoes single electron reduction *via* electron transfer from DIPEA, generating the desired radical **Mes-Acr•**. To chemically probe the

possibility of charge transfer to the *N*-phenyl ring, brominated acridinium **1** was prepared. In the presence of 3 eq. DIPEA, **1** was completely converted to a mixture of debrominated acridinum **1a** and hydroacridine **1b** following irradiation at 390 nm for 18 hours (Figure 1F). As aryl halide radical anions are known to quickly fragment to yield the corresponding aryl radicals, this experiment is indicative of the formation of radical anion character localized on the *N*-phenyl ring during excitation.

To evaluate the competency of this radical species as a catalytic reductant, conditions for the reductive dehalogenation of aryl halides were developed (Figure 2A). A variety of both electron-rich (**6–13**) and electron-poor (**14, 15**) aryl bromides afforded the desired hydrodebrominated products in good to excellent yields (NMR yields of products taken using HMDSO as an internal standard). It is of note that reductively recalcitrant aryl chlorides also participated efficiently in this reaction, in contrast to previously reported methods which are only effective for electron-poor (under visible light irradiation) or moderately electron rich aryl chlorides (under UVA irradiation).[31,32] A variety of both electron-donating (**16–20)** and electron-withdrawing (**21–24**) substituents were tolerated, with only slightly reduced yields in the case of electron-poor substrates. Substrates bearing ketone (**30**), carboxylic acid (**31**), and alcohol (**28**) functionalities all afforded the desired hydrodechlorinated products in good to excellent yield. Medicinally relevant pyridine (**25, 26**) and aryl carbamate (**27**) derivatives were also efficient substrates for this transformation. When substrate (**23**), which bears a trifluoromethyl substituent, was subjected to the reaction conditions, partial hydrodefluorination (5%) to yield the corresponding difluoromethyl derivative was observed in addition to hydrodechlorination. In all other examples, no Birch-type products resulting from overreduction are detected. The *bis*-reduction of polyhalogenated compounds (**9a**) and (**9b**) gave the corresponding *bis*-hydrodebromination (**9**) and *bis*-hydrodechlorination products in 58% yield and 46% yield, respectively. For compound **9b**, 49% yield of the product resulting from *mono*-hydrodechlorination (**9c**) was observed in addition to the fully dechlorinated product.

Based on prior work in reductive dehalogenation, the following mechanism is proposed (Figure 2B). Following excitation, **Mes-Acr^{+}BF$_4^{-}$** engages in single electron transfer with the tertiary amine reductant (**DIPEA**), generating **Mes-Acr•** and the corresponding amine cation radical. **Mes-Acr•** is then excited by 390 nm light, populating a combination of highly reducing D_n/**TICT** excited states, and undergoes electron transfer with an electronically matched aryl halide generating an arene radical anion and reforming **Mes-Acr^{+}BF$_4^{-}$**. The arene radical anion then fragments yielding an aryl radical. The resulting aryl radical abstracts a hydrogen atom from the amine cation radical, yielding the desired product as well as the corresponding iminium salt. Deuterium labeling studies confirmed the amine cation radical as the primary source of hydrogen atoms in this system (see SI – no deuterium incorporation in MeCN-d3).

The reductive detosylation of amines was identified as another possible transformation, which may be facilitated by **Mes-Acr•** (Figure 3). Typically, strong acid, dissolving metal (Li/Mg), or low-valent transition metal reductions are employed in detosylation reactions.[33–35] A variety of electronically diverse tosylated aniline derivatives were smoothly converted to the desired free anilines in moderate to excellent yield. Interestingly, substrates

containing aryl halides were tolerated under the reaction conditions. As this reaction is conducted at a significantly lower concentration of substrate compared to the reductive dehalogenation method (0.1 M vs. 0.5 M), the observed lack of aryl halide reduction may be a function of concentration. Esters (**43, 73**), free carboxylic acids (**44**), ketones (**48**), and free alcohols (**58**) were tolerated under the reaction conditions, showcasing the high functional group tolerance of this method relative to methods relying on harsh dissolving metal conditions. Benzylic (**52**) and secondary alkyl amines (**45, 53, 65–68**) were efficient substrates for this transformation as well. Medicinally-relevant heterocycles, including pyridines (**59**), indoles (**58**), pyrroles (**62**), pyrrolidines (**67**), indazoles (**63**), benzimidazoles (**64**), and morpholines (**65**) were deprotected in good to excellent yields, with no reduction of the aromatic system observed in all cases. Of note is the ability of this method to chemoselectively and efficiently deprotect tosyl-amines over mesyl protected-amines, as shown by the reaction of substrate **51**, yielding the desired detosylation product in 61% yield with no observed cleavage of the mesyl-amine. Additionally, the reaction performed well on 1.28 g scale, with substrate **64** undergoing the desired detosylation in 92% yield when conducted in a standard round bottom flask irradiated with LED lamps (see SI for experimental details).

In conclusion, an acridine radical generated *in situ* from single electron reduction of an acridinium derivative may act as potent single electron reductant upon excitation with 390 nm light. Spectroscopic and computational investigations indicate the formation of at least two distinct excited states, one of which may be characterized as a TICT state. The development of chemoselective dehalogenation and desulfonylation reactions utilizing **Mes-Acr•** compliment the well-known oxidative chemistry associated with acridinium salts and highlight the potential for the development of other types of reactions based on excitation of organic radicals.

Supplementary Material

Refer to Web version on PubMed Central for supplementary material.

Acknowledgements:

This work was supported in part by the National Institutes of Health (NIGMS) Award No. R01 GM120186 (D.A.N.). L.F.W. was supported by the National Natural Science Foundation of China (21801011) and the International Postdoctoral Exchange Fellowship Program (20180033). O.F.W. and A.M. were supported by the National Science Foundation under CHE-1763207. Photophysical measurements were performed in the AMPED EFRC Instrumentation Facility established by the Alliance for Molecular PhotoElectrode Design for Solar Fuels (AMPED), an Energy Frontier Research Center (EFRC) funded by the U.S. Department of Energy, Office of Science, Office of Basic Energy Sciences under Award DE-SC0001011. B.D.D acknowledges support for this project by the Department of Energy (DOE)- Basic Energy Sciences through the Chemical Sciences Geosciences and Biosciences Division, through grant no. DE- SC0016501.

References:

1. Mattay J Photoinduced Electron Transfer in Organic Synthesis. Synthesis 1989, 233–252 (1989).
2. Bauer A, Westkämper F, Grimme S & Bach T Catalytic enantioselective reactions driven by photoinduced electron transfer. Nature 436, 1139–1140 (2005). [PubMed: 16121176]
3. Fox MA Photoinduced Electron Transfer. Photochem. Photobiol 52, 617–627 (1990).

4. Fukuzumi S New development of photoinduced electron-transfer catalytic systems. Pure Appl. Chem 79, 981–991 (2007).
5. Romero NA & Nicewicz DA Organic Photoredox Catalysis. Chem. Rev 116, 10075–10166 (2016). [PubMed: 27285582]
6. Prier CK, Rankic DA & MacMillan DWC Visible Light Photoredox Catalysis with Transition Metal Complexes: Applications in Organic Synthesis. Chem. Rev 113, 5322–5363 (2013). [PubMed: 23509883]
7. Johnston LJ Photochemistry of radicals and biradicals. Chem. Rev 93, 251–266 (1993).
8. Arnold BR, Scaiano JC & McGimpsey WG Electron-transfer quenching of excited diphenylmethyl radicals. J. Am. Chem. Soc 114, 9978–9982 (1992).
9. Scaiano JC, Tanner M & Weir D Exploratory study of the intermolecular reactivity of excited diphenylmethyl radicals. J. Am. Chem. Soc 107, 4396–4403 (1985).
10. Samanta A Bhattacharyya K, Das PK, Kamat PV, Weir D, Hug GL Quenching of excited doublet states of organic radicals by stable radicals. J. Phys. Chem 93, 3651–3656 (1989).
11. Weir D & Scaiano JC Substituent effects on the lifetime and fluorescence of excited diphenylmethyl radicals in solution. Chem. Phys. Lett 128, 156–159 (1986).
12. Scordilis-Kelley C Alkali Metal Reduction Potentials Measured in Chloroaluminate Ambient-Temperature Molten Salts. J. Electrochem. Soc 139, 694 (1992).
13. Margrey KA & Nicewicz DA A General Approach to Catalytic Alkene Anti-Markovnikov Hydrofunctionalization Reactions via Acridinium Photoredox Catalysis. Acc. Chem. Res 49, 1997–2006 (2016). [PubMed: 27588818]
14. Romero NA & Nicewicz DA Mechanistic Insight into the Photoredox Catalysis of Anti-Markovnikov Alkene Hydrofunctionalization Reactions. J. Am. Chem. Soc 136, 17024–17035 (2014). [PubMed: 25390821]
15. Ghosh I, Ghosh T, Bardagi JI & König B Reduction of aryl halides by consecutive visible light-induced electron transfer processes. Science 346, 725–728 (2014). [PubMed: 25378618]
16. Connell TU, Fraser CL, Czyz ML, Smith ZM, Hayne DJ, Doeven EH, Agugiaro J, Wilson DJD, Adcock JL, Scully AD, Gómez DE, Barnett NW, Polyzos A & Francis PS The Tandem Photoredox Catalysis Mechanism of [Ir(ppy)2(dtb-bpy)]+ Enabling Access to Energy Demanding Organic Substrates. J. Am. Chem. Soc 141, 17646–17658 (2019). [PubMed: 31545022]
17. Lu C, Fujitsuka M, Sugimoto A & Majima T Dual Character of Excited Radical Anions in Aromatic Diimide Bis(radical anion)s: Donor or Acceptor? J. Phys. Chem C 121, 4558–4563 (2017).
18. Christensen JA et al. Phenothiazine Radical Cation Excited States as Super-oxidants for Energy-Demanding Reactions. J. Am. Chem. Soc 140, 5290–5299 (2018). [PubMed: 29589754]
19. Gumy J-C & Vauthey E Investigation of the Excited-State Dynamics of Radical Ions in the Condensed Phase Using the Picosecond Transient Grating Technique. J. Phys. Chem. A 101, 8575–8580 (1997).
20. Brancato G, Signore G, Neyroz P, Polli D, Cerullo G, Abbandonato G, Nucara L, Barone V, Beltram F & Bizzarri R Dual Fluorescence through Kasha's Rule Breaking: An Unconventional Photomechanism for Intracellular Probe Design. J. Phys. Chem. B 119, 6144–6154 (2015). [PubMed: 25902266]
21. Demchenko AP, Tomin VI & Chou P-T Breaking the Kasha Rule for More Efficient Photochemistry. Chem. Rev 117, 13353–13381 (2017). [PubMed: 28991479]
22. Peng Z Wang Z, Huang Z, Liu S, Lu P & Wang Y Expression of anti-Kasha's emission from amino benzothiadiazole and its utilization for fluorescent chemosensors and organic light emitting materials. J. Mater. Chem C 6, 7864–7873 (2018).
23. Scuppa S, Orian L, Donoli A, Santi S & Meneghetti M Anti-Kasha's Rule Fluorescence Emission in (2-Ferrocenyl)indene Generated by a Twisted Intramolecular Charge-Transfer (TICT) Process. J. Phys. Chem. A 115, 8344–8349 (2011). [PubMed: 21692524]
24. Romero NA, Margrey KA, Tay NE & Nicewicz DA Site-selective arene C-H amination via photoredox catalysis. Science 349, 1326–1330 (2015). [PubMed: 26383949]
25. Bhandari S & Dunietz BD Quantitative Accuracy in Calculating Charge Transfer State Energies in Solvated Molecular Complexes Using a Screened Range Separated Hybrid Functional within a

Polarized Continuum Model. J. Chem. Theory Comput 15, 4305–4311 (2019). [PubMed: 31356067]

26. Song Y Schubert A, Maret E, Burdick RK, Dunietz BD, Geva E, Ogilvie JP Vibronic structure of photosynthetic pigments probed by polarized two-dimensional electronic spectroscopy and ab initio calculations. Chem. Sci 10, 8143–8153 (2019). [PubMed: 31857881]
27. Bhandari S, Cheung MS, Geva E, Kronik L & Dunietz BD Fundamental Gaps of Condensed-Phase Organic Semiconductors from Single-Molecule Calculations using Polarization-Consistent Optimally Tuned Screened Range-Separated Hybrid Functionals. J. Chem. Theory Comput 14, 6287–6294 (2018). [PubMed: 30444365]
28. Maiti B, Schubert A, Sarkar S, Bhandari S, Wang K, Li Z, Geva E, Twieg RJ & Dunietz BD, Enhancing charge mobilities in organic semiconductors by selective fluorination: a design approach based on a quantum mechanical perspective. Chem. Sci 8, 6947–6953 (2017). [PubMed: 29147520]
29. Shida T Electronic Absorption Spectra of Radical Ions. (Elsevier, 1988).
30. Kerzig C & Goez M Generating hydrated electrons through photoredox catalysis with 9-anthrolate. Phys. Chem. Chem. Phys 17, 13829–13836 (2015). [PubMed: 25929856]
31. Kerzig C, Guo X & Wenger OS Unexpected Hydrated Electron Source for Preparative Visible-Light Driven Photoredox Catalysis. J. Am. Chem. Soc 141, 2122–2127 (2019). [PubMed: 30672694]
32. Poelma SO, Burnett GL, Discekici EH, Mattson KM, Treat NJ, Luo Y, Hudson ZM, Shankel SL, Clark PG, Kramer JK, Hawker CJ & Read de Alaniz J Chemoselective Radical Dehalogenation and C–C Bond Formation on Aryl Halide Substrates Using Organic Photoredox Catalysts. J. Org. Chem 81, 7155–7160 (2016). [PubMed: 27276418]
33. Discekici EH Treat NJ, Poelma SO, Mattson KM, Hudson ZM, Luo Y, Hawker CJ & Read de Alaniz J A highly reducing metal-free photoredox catalyst: design and application in radical dehalogenations. Chem. Commun 51, 11705–11708 (2015).
34. Narayanam JMR, Tucker JW & Stephenson CRJ Electron-Transfer Photoredox Catalysis: Development of a Tin-Free Reductive Dehalogenation Reaction. J. Am. Chem. Soc 131, 8756–8757 (2009). [PubMed: 19552447]
35. Yin H, Jin Y, Hertzog JE, Mullane KC, Carroll PJ, Manor BC, Anna JM & Schelter EJ The Hexachlorocerate(III) Anion: A Potent, Benchtop Stable, and Readily Available Ultraviolet A Photosensitizer for Aryl Chlorides. J. Am. Chem. Soc 138, 16266–16273 (2016). [PubMed: 27936638]
36. Poelma SO, Burnett GL, Discekici EH, Mattson KM, Treat NJ, Luo Y, Hudson ZM, Shankel SL, Clark PG, Kramer JK, Hawker CJ & Read de Alaniz J Chemoselective Radical Dehalogenation and C–C Bond Formation on Aryl Halide Substrates Using Organic Photoredox Catalysts. J. Org. Chem 81, 7155–7160 (2016). [PubMed: 27276418]
37. Javorskis T & Orentas E Chemoselective Deprotection of Sulfonamides Under Acidic Conditions: Scope, Sulfonyl Group Migration, and Synthetic Applications. J. Org. Chem 82, 13423–13439 (2017). [PubMed: 29206042]
38. Shohji N, Kawaji T & Okamoto S Ti(O-i-Pr)4/Me3SiCl/Mg-Mediated Reductive Cleavage of Sulfonamides and Sulfonates to Amines and Alcohols. Org. Lett 13, 2626–2629 (2011). [PubMed: 21510616]
39. Alonso E, Ramón DJ & Yus M Reductive deprotection of allyl, benzyl and sulfonyl substituted alcohols, amines and amides using a naphthalene-catalysed lithiation. Tetrahedron 53, 14355–14368 (1997).

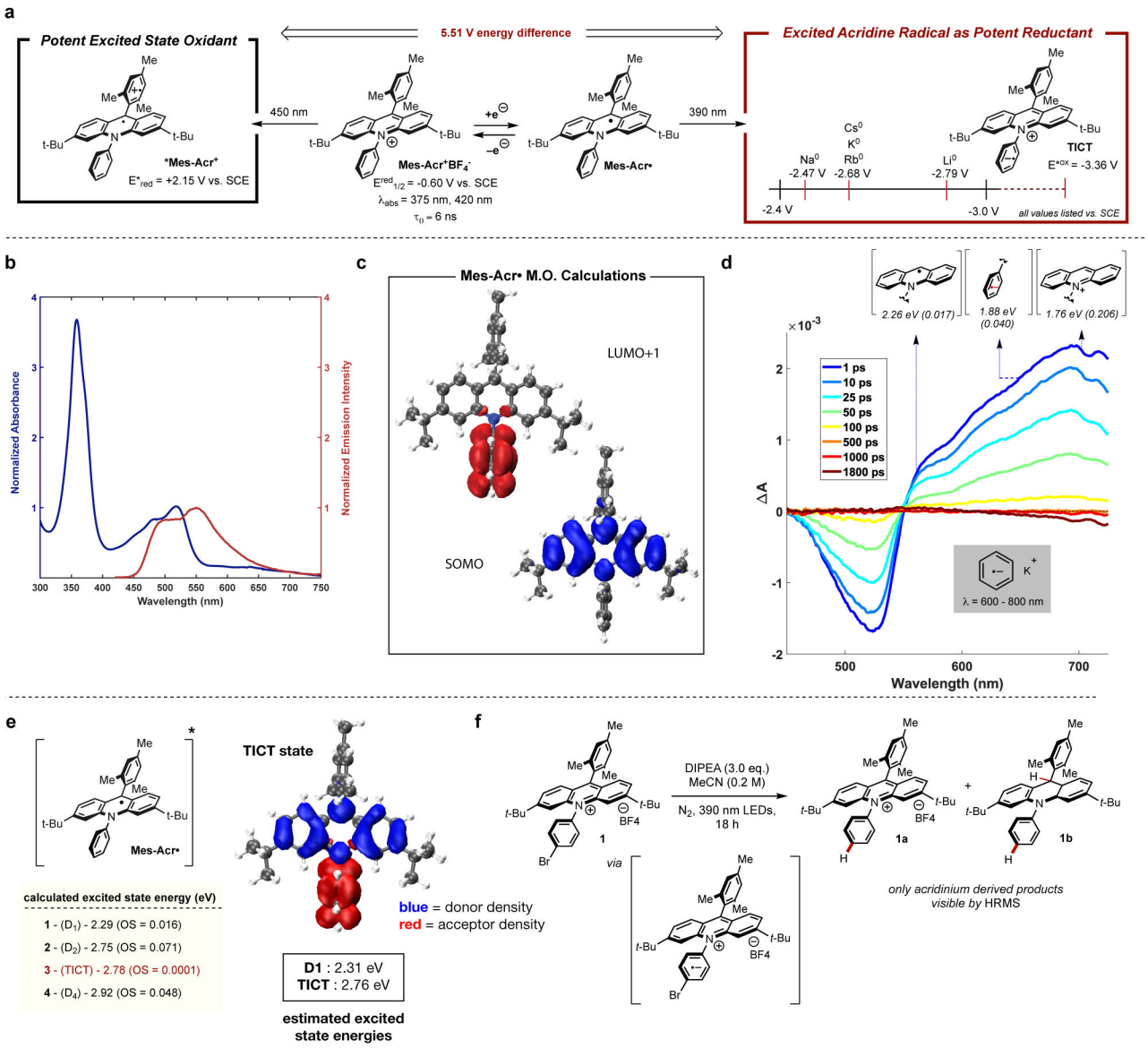

Figure 1: Mechanistic studies on Mes-Acr radical.

a, Reduction potential of various elemental alkali metals compared to peak reducing potential of Mes-Acr•, **b**, Absorbance and emission (excitation = 400 nm) profiles for Mes-Acr• in MeCN (5 mM, 1 mm path length) **c**, SOMO and LUMO +1 visualizations for **Mes-Acr•**. **d**, Transient absorption spectra of **Mes-Acr•** (2.5 mM, THF, 1 mm path length) collected with a 250 fs pump pulse centered at 400 nm **e**, Excited state energies calculated using SRSH-PCM/TD-DFT method for **Mes-Acr•** and frontier orbital plot showing donor and acceptor density for **TICT** excited state. **f**, Debromination reaction of brominated acridinium derivative giving circumstantial evidence for **TICT** state. Mes = mesityl; DIPEA = *N,N*-diisopropylethylamine; *t*-Bu = tert-butyl.

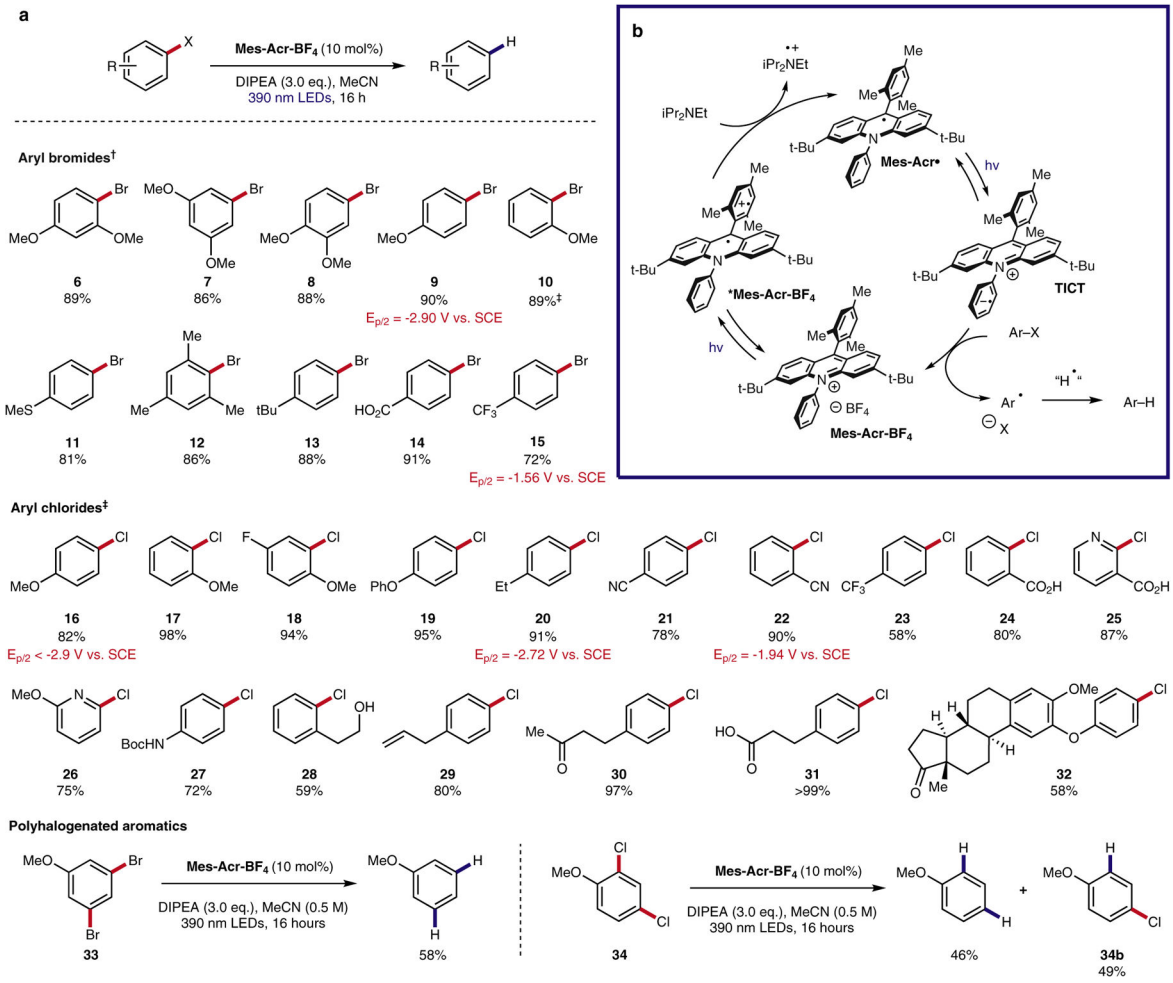

Figure 2: Reductive dehalogenation of aryl halides enabled by acridine radical photoredox catalysis

a, Reaction scope. **b**, proposed mechanism. †0.3 M reaction concentration. ‡0.5 M reaction concentration.

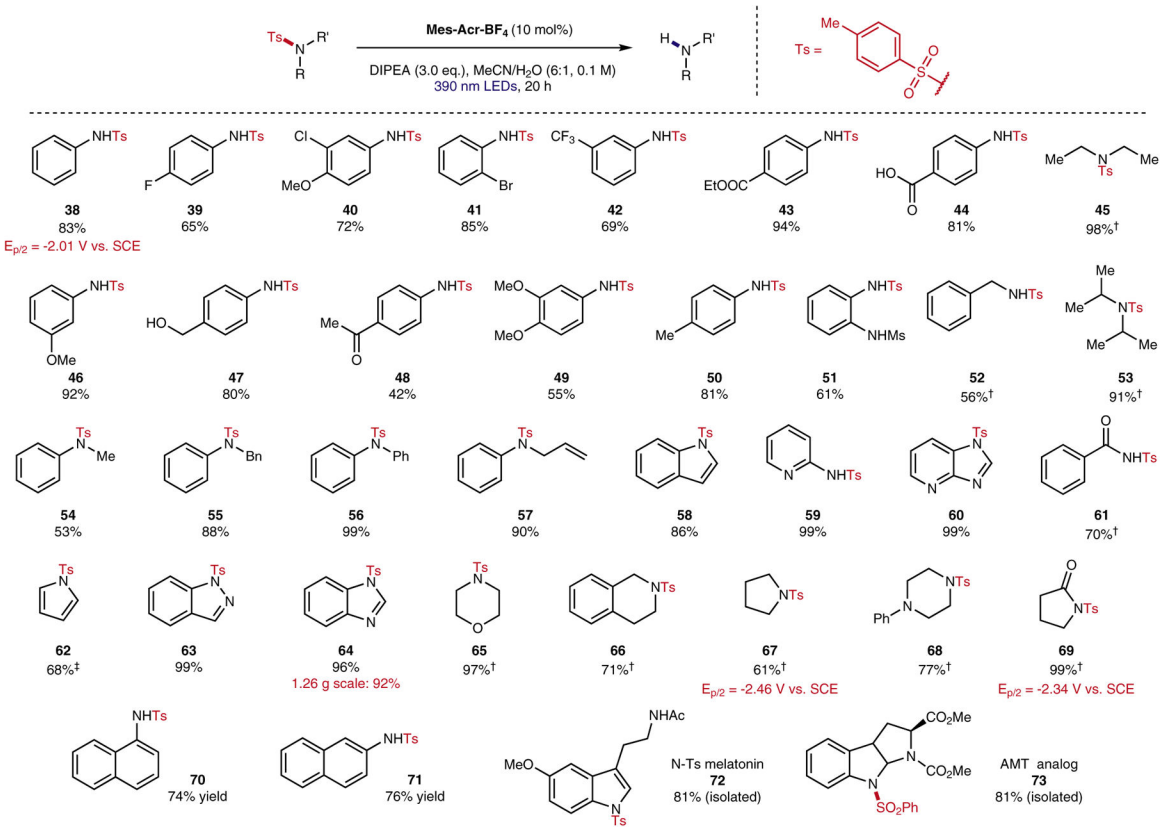

Figure 3: Scope of reductive detosylation catalyzed by Mes-Acr•.

^{1}H NMR yields using DMSO or pyrazine as internal standard. †48 h reaction time. ‡0.5 M reaction concentration. Ts = *p*-toluenesulfonyl